PICKUP COMETARY IONS AT COMET 67P/C-G: COMPARISON OF TEST PARTICLE MODELS WITH ROSETTA IES DATA. A. Rahmati[1], T. E. Cravens[1], H. Madanian[1], J. L. Burch[2], R. Goldstein[2], and the Rosetta IES team. [1]Department of Physics and Astronomy, University of Kansas, Lawrence, KS, [2]Southwest Research Institute, San Antonio, TX.

Introduction: The Rosetta mission to Comet 67P/Churyumov-Gerasimenko, marks the first extensive study of a cometary plasma environment, beginning with low cometary activity, when the spacecraft rendezvoused with the comet on August 6, 2014. At the time of the arrival of Rosetta, the comet was at a heliocentric distance of 3.6 AU from the Sun, and on Jan 1, 2015, the comet was at 2.6 AU. For these distances, the production rate of H_2O from the comet ranged between 10^{26} to 10^{27} s^{-1}, and a weak interaction between the solar wind and the cometary neutral coma is predicted [1]. The Ion and Electron Sensor (IES) onboard Rosetta is designed to study the solar wind electrons and ions as well as the cometary plasma [2]. IES measures the flux of electrons and ions with an energy/charge range of 5 eV/e to 20 keV/e and a field of view of 2.8π sr. In this work we construct a Haser model [3] of the neutral coma of the comet and calculate the flux and density of the heavy pickup cometary ions with a test particle code [4, 5] and compare our results with IES data.

Model and Results: We use a Haser model to construct a spherically symmetric neutral coma of the comet at ~3 AU. The comet is assumed to have an H_2O production rate of 10^{26} s^{-1} and an outflow velocity of 1 km/s. The dissociation frequency of H_2O is assumed to be 10^{-6} s^{-1}. Figure 1 shows the neutral densities predicted by the Haser model for both the parent (H_2O) and the daughter (H, OH) species. OH will also in turn dissociate into H and O, but the granddaughter densities will only become comparable to their parent densities at distances greater than 10^6 km; therefore, we did not include them in our simulations. Peak H_2O density of 10^8 cm^{-3} near the surface of the comet is predicted.

Ionization of the major neutral species will create ions that are picked up by the solar wind magnetic and motional electric fields. A test particle code tracks the trajectories of H_2O^+ ions and calculates the pickup ion fluxes and densities near the comet. Figure 2 shows the differential energy flux of H_2O^+ pickup ions 30 km upstream of the comet. A solar wind velocity of 400 km/s with a magnetic field of 1 nT, perpendicular to the solar wind bulk flow direction is assumed. The ionization frequency for water molecules is assumed to be 10^{-7} s^{-1}. Peak pickup ion differential energy flux of ~10^6 eV/cm^2-s-eV at low energies is predicted.

Due to the very large gyro-radius of the heavy ions (~ 10^5 km), most of the ions near the comet are newly born and have low energies. Figure 3 shows the density of pickup ions near the comet calculated by the test particle code. At 30 km upstream of the comet (x=30 km, z=0), the H_2O^+ density is ~5 cm^{-3}, which is about an order of magnitude higher than the solar wind density at 3 AU. The newly born pickup ions begin their trajectory parallel to the solar wind motional electric field, which is on the order of 0.5 V/km for an undisturbed solar wind at 3 AU. Therefore, most of the pickup ions in the vicinity of the comet (r<50 km) have energies below 30 eV. Thus, a negative spacecraft potential can easily accelerate these newly born ions toward the spacecraft, such that the IES instrument detects them in its lower energy channels.

Figure 4 shows a typical spectrogram for the ion mode of IES, for November 10, 2014, when the comet was at 3 AU and the spacecraft was at a distance of 30 km from the comet. In this spectrogram, the solar wind protons (H^+) and alpha particles (He^{++}) are detected at energy/charge channels of 1600 and 3200 eV/e, respectively. The count-rates seen near the lower end of the energy spectrum (~20 V) are the accelerated pickup ions due to the negative spacecraft charging.

Figure 5 is a polar plot for the same day for hours 08:00 to 10:00 and elevations 4-5. The plot is of energy flux vs. energy and azimuth (anode) with the zero azimuth at +x and going counterclockwise. IES has 16 elevations and 16 anodes; however, for some of the instrument modes the adjacent bins are first averaged and then transmitted due to data downlink constraints. The solar wind ions are seen at the 2nd quadrant of the polar plot and the low energy pickup ions are detected at most of the elevations/azimuths, meaning they were pulled into the detector due to the negative charging of the spacecraft.

In this work we model the anticipated IES countrates for heavy pickup ions accelerated by a combination of the solar wind motional electric field and the negative charging of the spacecraft. We compare our results with the IES measured counts.

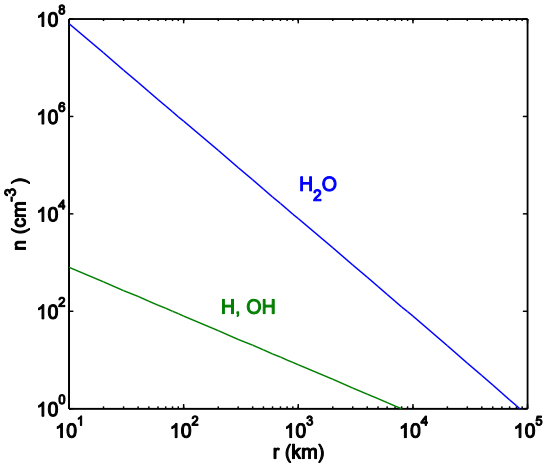

Figure 1. Neutral density profile of the cometary coma at ~3 AU for a production rate of 10^{26} s^{-1}. Parent (H_2O) and daughter (H, OH) densities are constructed using a Haser model of the coma.

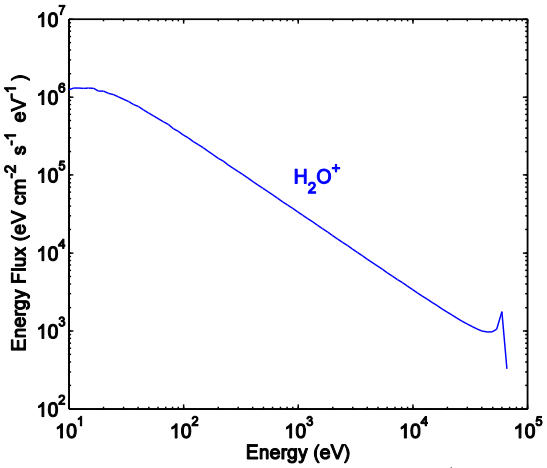

Figure 2. Differential energy flux of H_2O^+ ions calculated by the test particle code.

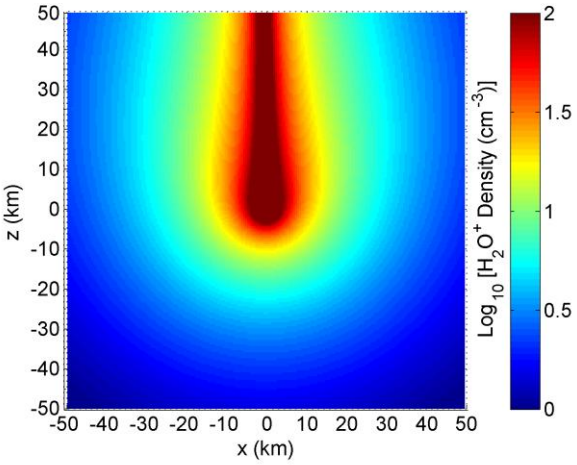

Figure 3. Density of H_2O^+ near the comet calculated by the test particle code, shown in Log_{10} [n_{H2O+} (cm^{-3})].

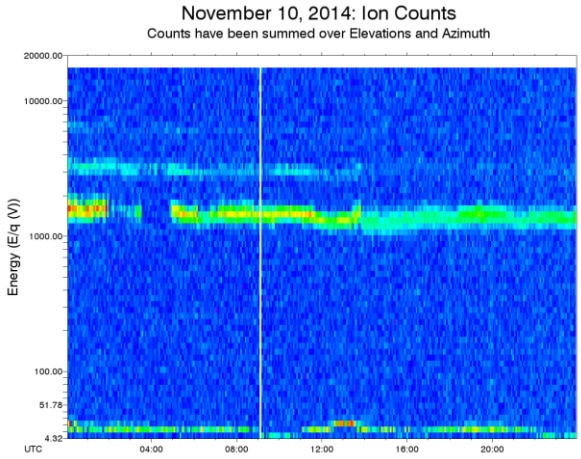

Figure 4. Energy spectrogram measured by IES showing the solar wind protons and alpha particles, as well as the low energy counts corresponding to the newly born pickup ions pulled into the detector due to the negative charging of the spacecraft.

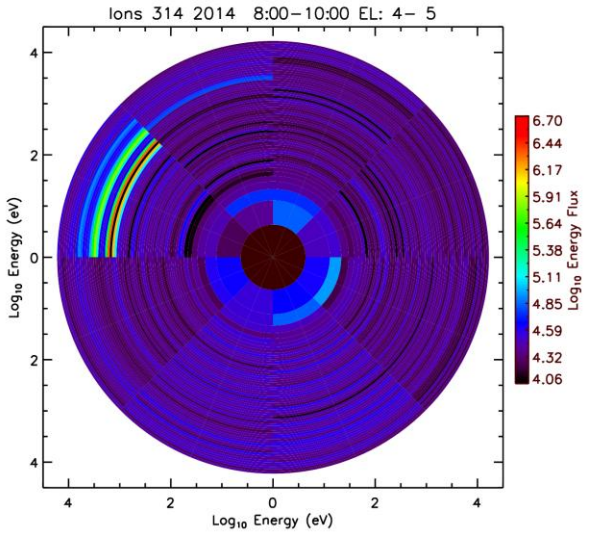

Figure 5. Polar plot for November 10, 2014, hours 08:00 to 10:00 for elevations 4-5. The plot is of energy flux vs. energy and azimuth with the zero azimuth at +x and going counterclockwise. Solar wind ions are at the 2nd quadrant. Low-energy pickup ions are seen at most of the elevations/azimuths.

References:

[1] Rubin M. et al. (2014) *Icarus 242*, 38-49 [2] Burch J. L. et al. (2007) *Space Sci. Rev. 128*, 697-712 [3] Haser L. (1957) *Bull. Acad. R. d Belgique, Classe de Sci. 34(5)*, 740-750 [4] Cravens T. E. et al. (2002) *JGR, 107*, A8 [5] Rahmati A. et al. (2014) *GRL 41(14)*, 4812-4818.